Electrical/Magnetic Properties of Al/ Fe_2O_3 Laminated Composites

Saeed Daneshmand[1*], Luis Andres Barboza-Arenas[2], Assad A.H AlZubaidi[3], Jamal K. Abbas[4], M. Abdulfadhil Gatea[5]

1-Department of Mechanical Engineering, Isfahan (Khorasgan) Branch, Islamic Azad University, Isfahan, Iran.
Email S.daneshmand@iaumajlesi.ac.ir (Corresponding author)
2- Universidad Tecnológica del Perú, Perú.
E-mail: c20752@utp.edu.pe
3- Technical College of Engineering, Al-Bayan University, Baghdad, Iraq.
E-mail: asaad.a@albayan.edu.iq
4- AL-Nisour University College, Baghdad, Iraq.
Email: jamal.k.eng@nuc.edu.iq
5- Technical Engineering Department College of Technical Engineering, The Islamic University, Najaf, Iraq.
Email: maherab522@gmail.com

Received: 27 January 2023 Revised: 19 March 2023 Accepted: 19 May 2023

ABSTRACT:
To fabricate ultra-fine grain structures containing high strength, accumulative roll bonding is a kind of severe plastic deformation (SPD). In the present study, magnetic Al/ Fe_2O_3 composites reinforced with 0, 2.5% and 5Wt.% of Fe_2O_3 particles have been manufactured via ARB. A uniform distribution of Iron oxide particles was achieved after the 8^{th} cycles of ARB. Mechanical properties include (hardness, elongation, toughness) and also, magnetic and electrical properties such as magnetic saturation, magnetic permeability and magnetic residuals were studied. The presence of Fe_2O_3 particles improved the mechanical, electrical and magnetic properties of this kind of laminated composites. Vibrating sample magnetometer was utilized to study the magnetic properties of samples vs No. of steps.

KEYWORDS: Accumulative Roll Bonding, Magnetic Properties, Electrical Conductivity, Laminated Composites.

1. INTRODUCTION

In recent years, there are many advances in electrical engineering, electrical devices in many fields such as military, aerospace, vessels, machines and etc. which needs high values of magnetic fields. All of these needs utilizing of materials including high capacities of materials with high electrical conductivity, low electrical resistivity with propeller magnetic properties and suitable costs [1-5]. To this purpose, many investigations have been done on the metal matrix composites (MMCs) [6-13]. Generation of ultra-fine grain materials is a new novel technique to improve the mechanical properties of MMCs. Vice versa other forming process to generate UFG material structure by means of this process, having of good mechanical and ductility of a MMCs is available. Hall petch relation explains the relation between the grain size of the crystalline lattice and the strength of materials and is as:

$$\sigma_Y = \sigma_0 + kd^{\frac{-1}{2}} \quad (1)$$

Where σ_Y, σ_0, d and k are yield strength, ultimate tensile strength and a constant relates to the kind of materials, respectively. Based on Eq.1, the strength of materials increases by decreasing the grain size of crystalline structure. SPD deformation techniques usually decrease the grain size of structure and is done by applying very high values of plastic strain on materials [14-20]. Usually, structure change due to SPD techniques can leads to generation of Nano structure with different electrical and chemical properties. ARB process is a new novel technique to fabricate MMCs which is proposed by Saito et al. at 1998 for the first time [21-25]. Based on this process, rolling is conducted on strips with unchangeable width and length with a 50% reduction thickness in each pass. The benefit of this process is the ability to create UFG structure in comparison with other industrial processes. So, this process is used recently to fabricate MMCs with desirable electrical and magnetic properties [26-32]. In many investigations usually a metal or ally is

Paper type: Research paper
DOI: 10.30486/mjee.2023.1976509.1042
How to cite this paper: S. Daneshmand, L. A. Barboza-Arenas, A. A.H AlZubaidi, J. K. Abbas and M. Abdulfadhil Gatea, **"Electrical/Magnetic Properties of Al/ Fe2O3 Laminated Composites"**, *Majlesi Journal of Electrical Engineering*, Vol. 17, No. 2, pp. 91-97, 2023.

used to fabricate multilayered laminates and in this study Fe_2O_3 particles are used as reinforcement to improve the mechanical, electrical and magnetic properties in this kind of composites. It is necessary to highlight the use of Fe_3O_4-based NPs in emerging applications, such as biomedical applications (hyperthermia, MRI contrast agents, and drug delivery), biosensing, environmental applications for the removal of heavy metals and organic pollutants, and applications in energy storage devices. During recent years, it is tried to improve the magnetic properties of composites. Usually, a metal has a definite property and by fabrication of composites, it is available to get various properties together [30-33]. So, in this approach, fabrication of a MMC with high prominent magnetic properties is needed. Aluminum has good electrical conductivity, heat conductivity and is a diamagnetic metal. Iron oxide is a ferromagnetic and shows a super paramagnetic reaction. By inserting iron oxides (Fe_2O_3) between Al layers in this kind of multilayered composites, a UFG composite with high magnetic properties is achieved. The main goal of this research is to fabricate the Al/ Fe_2O_3 composite vs ARB process and study of their mechanical, electrical and magnetic properties which is done for the first time as its novelty. The results showed that by using ARB process, all of mechanical, electrical and magnetic properties of these composites improved and this is the novelty in this investigation.

2. TECHNICAL WORK PREPARATION

The raw materials used in this study are aluminum alloys 1060 with primary dimensions of 80×300 mm. A schematic diagram of the ARB process is illustrated in Fig. 1. Before beginning of ARB process, surface cleaning is vital to obtain an acceptable solid welding between layers. The composite samples were prepared in equivalent dimensions with acetone and dried at the ambient temperature. This is necessary to clean the contaminations from the metallic surfaces and generate a better metallic bonding. The uniform brushing of foils is necessary. Next, the two sheets were fastened at both ends with steel wires and were aligned and banned the samples from sliding under the rolling. They were then rolled with 50% of reduction in thickness ratio. The bi-layers sample was halved in the longitudinal direction, and the roll bonding was frequented. For next cumulative rolling steps, the reduction in thickness was again 50%. Thus, thin reinforced aluminum composite samples were produced by up to 6 rolling steps. With a thickness reduction of 50% and for each ARB step, the effective strain rate is 0.8 as:

$$\varepsilon_e = \frac{2}{\sqrt{3}} N ln \frac{t_0}{t} = \frac{2}{\sqrt{3}} ln \frac{1}{1-R} \quad (2)$$

In Eq. 1, R, ε_{eq}, t_0, N and t are reduction thickness, equivalent strain, No. of ARB pass, and thickness before and after ARB.

Fig. 1. Chart of ARB trial steps.

Sheets of annealed AA1050 with primary dimensions of 95 × 28 × 1 mm were primary strip samples. The contamination removal from the surfaces to be bonded is vital to generate a desirable bonding, Fig 2. As can be illustrated in Fig 2, these layers of composed of illuminations are dames against the creation of a successful metallic bonding. So, the surface preparation prior the rolling is necessary.

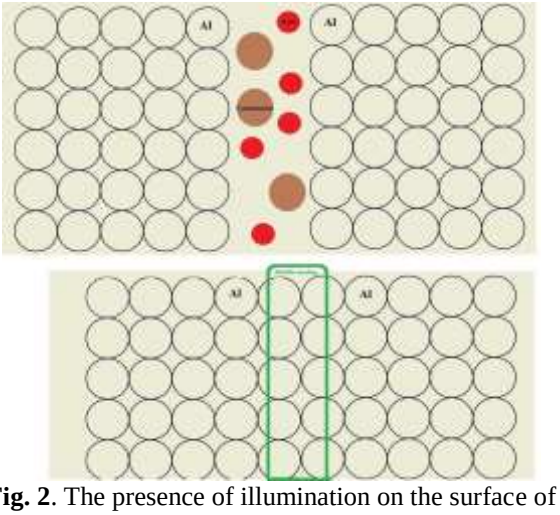

Fig. 2. The presence of illumination on the surface of samples before the bonding.

One Al strip and again the other of Al were slanted to get 2 mm thickness. Correct position of layers during the rolling is important. So, after stacking the composite samples with wires at ends, the samples were rolled under a 50% of thickness reduction for each cycle, respectively, Fig. 1. The ARB was continued up to eight cycles to generate a desirable scattering of Fe_2O_3 subdivisions in the Al matrix to study the effect of Fe_2O_3 Wt.% on the electro/magnetic and mechanical properties. So, the ARB cycles of the process are summarized in table 1. Fig. 3 shows the morphology of Fe_2O_3 particles which are used as a reinforcement through the Al matrix and effective parameter on the electro/ magnetic properties.

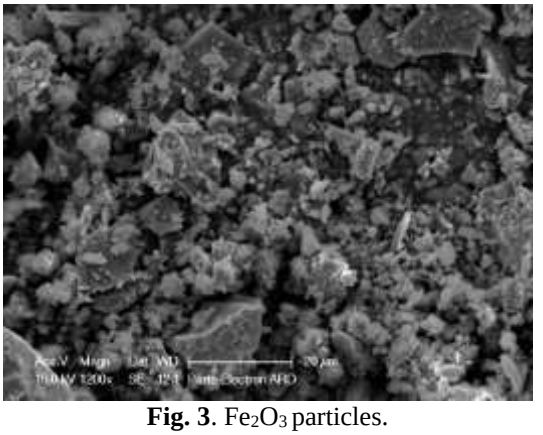

Fig. 3. Fe_2O_3 particles.

The magnetic saturation and magnetic residual tests and electrical conductivity were measured by using vibrating sample magnetometer. Fig. 4 shows the effective parameters on the hysteresis loop.

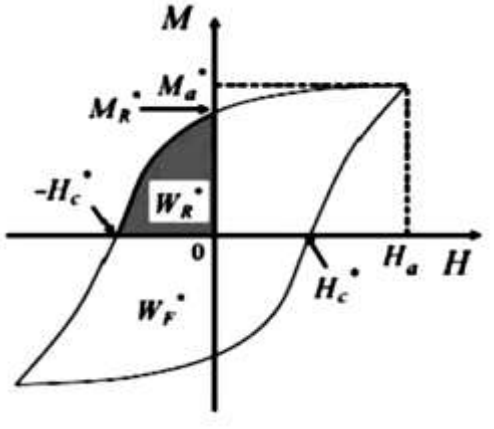

Fig. 4. Effective parameters on the hysteresis loop.

Table 1. Specifications of manufacturing process.

No. of cycles	No. of layers	No. of Fe_2O_3 layers
1	8	2
2	16	4
3	32	8
4	64	16
5	128	32
6	256	64
7	512	128
8	1024	256

A laboratory rolling machine with a capacity of 40 tones with a rotary speed of 60 rpm and roll diameter of 170 mm, is used in this study. ASTM standards E8M has been used to prepare composite samples for tensile test and also, ASTM-E384 for the Vickers hardness testing condition. The samples for wear test were in dimensions of 60×30×1mm with a rotary mechanism of ‘‘pin on disc’’ wear testing machine.

3. RESULTS

3.1. TENSILE STRENGTH

The strength of samples vs No. of passes is brought in Fig. 5 which is 76 and 158 for annealed Al and two passed sample, respectively. So, there is a rapid growth for the strength in this state. Then, this trend is approximately constant up to the final pass which gain the value of 160.1 MPa, Fig. 5. So, there are two increasing zones in Fig. 5 and the reason for both of them can be attributed to severe work hardening effect and creation of a UFG structure for zone (I) and then, local strain hardening of Al matrix around the Fe_2O_3 particles which is able to initiate slip systems [7, 23-26].

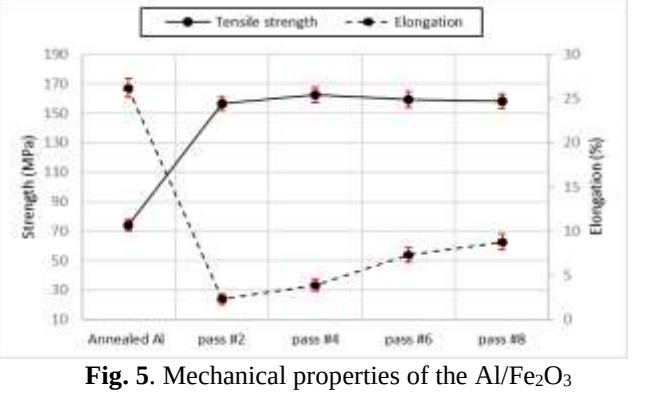

Fig. 5. Mechanical properties of the Al/Fe_2O_3 composites.

This trend for the elongation value is vice versa and is shown in Fig. 5. As can be seen in Fig. 5, there are also two same zones to explain the behavior of composites for elongation with mentioned explanations. The elongation value for annealed Al and samples with two and eight passes are 26.3%, 2.4% and 8.8%, respectively. It can be concluded that all the parameters that are effective on the strength behavior of composites are so valid here.

3. 2. HARDNESS TEST

Fig. 6. shows the variations of hardness value vs the No. of passes. According to Fig. 6, the average micro hardness improves up to pass#4 and then remains almost constant up to the final pass. Strain hardening and cumulating the dislocations density inside the crystalline lattice are two main factors for increasing of hardness at primary passes (less than the 4^{th} pass) and the other increasing in the second zone (between pass iously4 ad 8) is due to the local strain hardening around the iron oxide particles which is explained previously about the enhancement mechanism for strength.

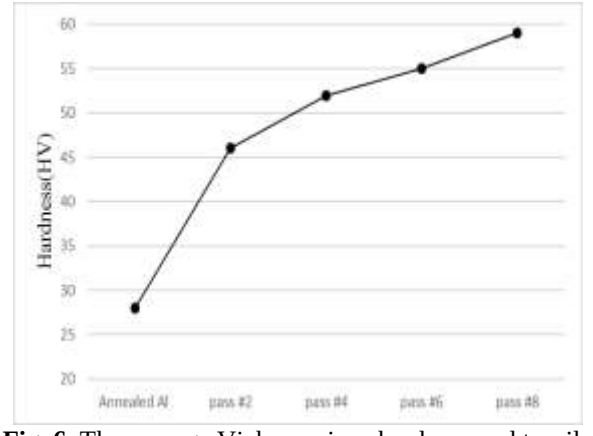

Fig. 6. The average Vickers micro-hardness and tensile toughness.

3.3. ELECTRICAL RESISTANCE

Fig. 7 shows the electrical resistivity of composite samples measured using four points probe method vs the number of cycles. The special resistivity constant of samples can be derived from Eq. 1.

$$\rho = G\frac{V}{I} = GR \quad (3)$$

In Eq. 1, ρ and R, are specific resistance and measured resistance of samples, respectively. Also, G is the corrective coefficient in the four-point probe method and can be derived as:

$$G = \frac{\pi}{Ln\ 2} tc\left(\frac{a}{d}.\frac{d}{s}\right) \quad (4)$$

Where, $\frac{\pi}{Ln\ 2}$, t and c are geometric factor, sample thickness and correction factor due to the rectangular shape of samples with length of a and width of b with a distance of s between the probes, respectively. Moreover, the electrical resistivity is the inverse of specific resistivity. The grain size has an essential effect on the resistivity due to the sub grain structure of the electricity flow surface of composite samples. Due to the flowing of electricity charge through a very thin surface of samples, there is a rapid increasing rate for the resistivity of composite samples from the annealed up to sample fabricated after the 8th steps. By increasing the number of steps up to eight, there is a slowing growth for the resistivity of samples due to the dynamic recrystallization of sample fabricated at 300 ^{o}C. Then, there is a rapid increasing rate for the resistivity after conducting a cold rolling step on the composite fabricated via eight ARB steps. This increasing rate is due to the generation of UFG structure in the Al matrix.

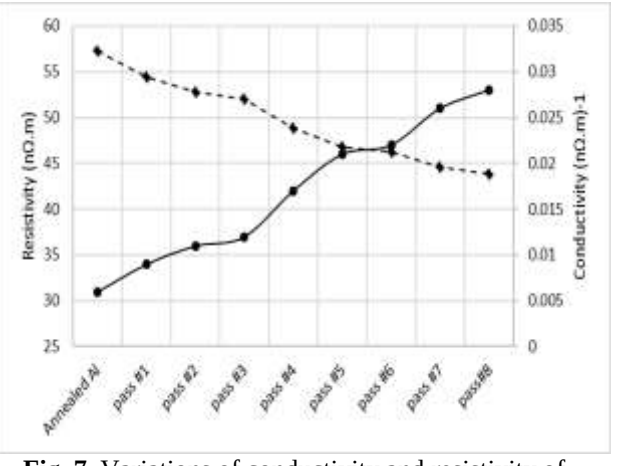

Fig. 7. Variations of conductivity and resistivity of composite samples vs the number of cycles.

The scattering of iron oxide particles through the Al matrix is shown in Fig. 8, which illustrates unvarying dispersal of iron oxides particles and small cluster. So, the porosities in the clusters are eliminated at higher amounts of plastic strain.

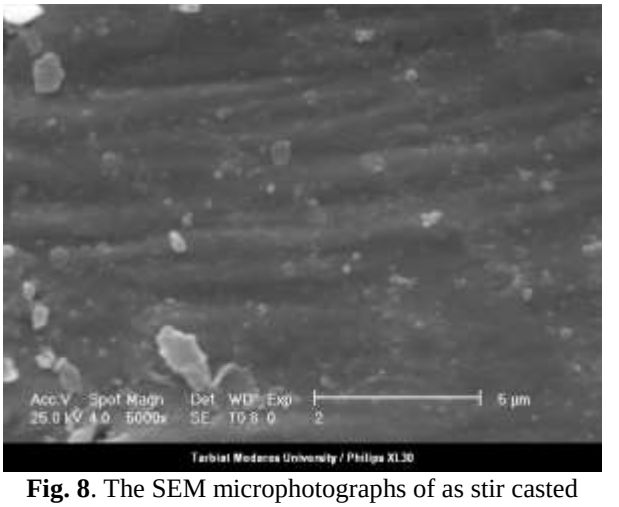

Fig. 8. The SEM microphotographs of as stir casted Al/TiO_2 composite.

For each cumulative rolling pass, if the reduction in thickness ratio was less than the threshold thickness reduction, metallic surfaces cannot bond together. The presence of iron oxide particles can improve this threshold value which is based on the energy barrier theory. For reductions more than this value, generation of a successful bonding is easy and that is impossible for values less than the threshold thickness reduction ratio.

3.4. MAGNETIC PROPERTIES

Figs. 9 and 10 show the hysteresis of composite samples fabricated via 2.5 and 5% of iron oxides vs different ARB passes. As can be seen in Fig. 9, the

residual magnetic values (M_R) are less than coercivity h_c charge values. Also, the iron oxide articles create a wider magnetic loop. This hard magnetic material has a wide magnetic loop and has high amounts of coercivity h_c charge. Also, this material resists to become a permanent magnet containing a low capacity of primary penetration. The penetration ability of a material means the ability to become a magnet through an external magnetic field. In these materials, orientation of the magnetic field zones does not change easily with the omission of the external magnetic field. On the other words, after omission of the external magnetic field, the hard magnetic materials keep their magnetic property. So, these materials are preferable to fabricate permanent magnets.

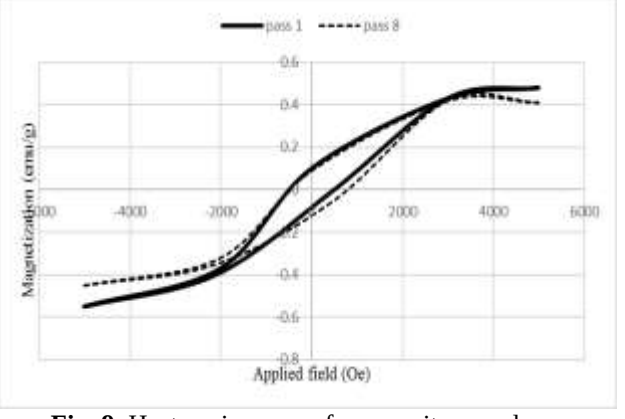

Fig. 9. Hysteresis curve of composite samples fabricated with 2.5% of Fe_2O_3 and after pass **(a)** one and **(b)** six.

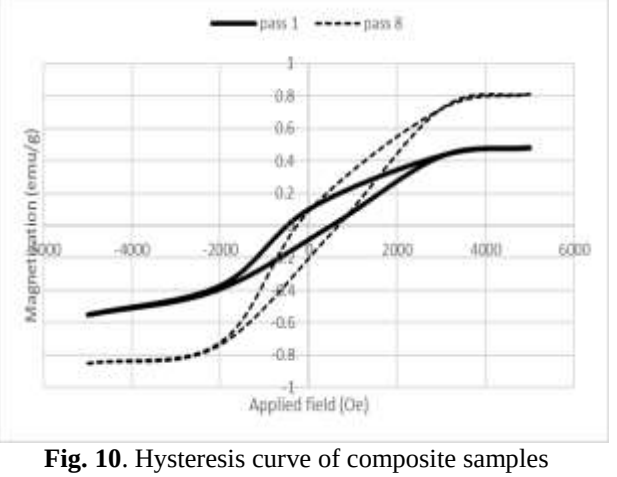

Fig. 10. Hysteresis curve of composite samples fabricated with **(a)** 2.5% and **(b)** 5% of Fe_2O_3 after eight pass of ARB.

According to Figs. 9 and 10, at higher passes of ARB, MR and hc improve with all of Al/ Fe_2O_3 composite samples. Increasing the both of these parameters has an essential effect on the improvement of magnetic property of composite samples.

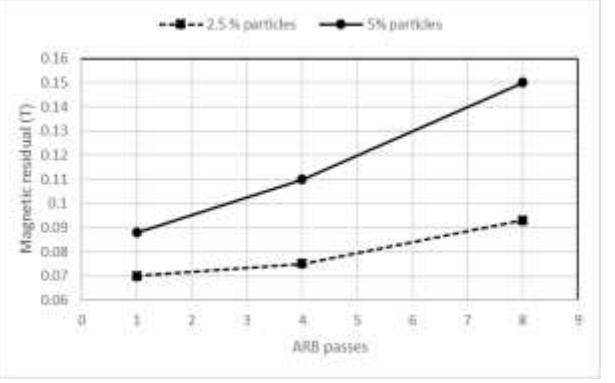

Fig. 9. Magnetic residual curve of composite samples vs ARB passes.

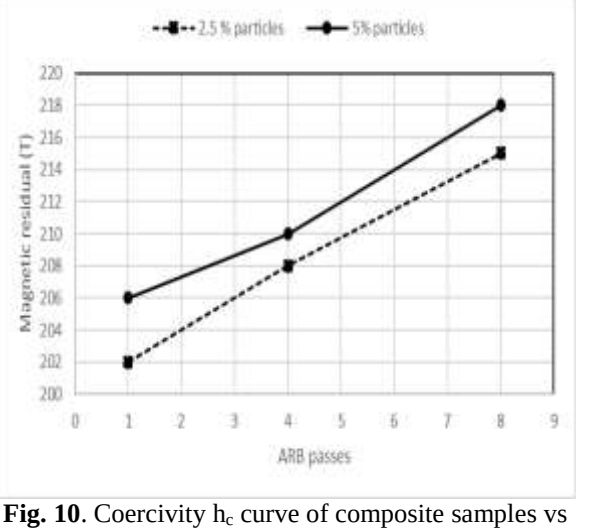

Fig. 10. Coercivity h_c curve of composite samples vs ARB passes.

As can be seen in Figs. 7-11, Fe_2O_3 particles can effectively enhance the magnetic properties of composite samples with Al matrix. In all samples, there are two states for magnetic saturation which is due to the poles positioning in unidirectional in opposite direction of the magnetic field which has its maximum value when magnetic dipoles are in the same direction with the external field.

As can be seen in Fig. 11, at higher number of ARB process, the magnetic saturation decreases due to the generation of force couple between adjacent atomic dipoles which deviates dipoles which position them in a reverse direction. This is due to the generation of ultra-fine grain (UFG) structure and increasing the number of grain boundaries through the Al matrix when decreases the magnetic saturation.

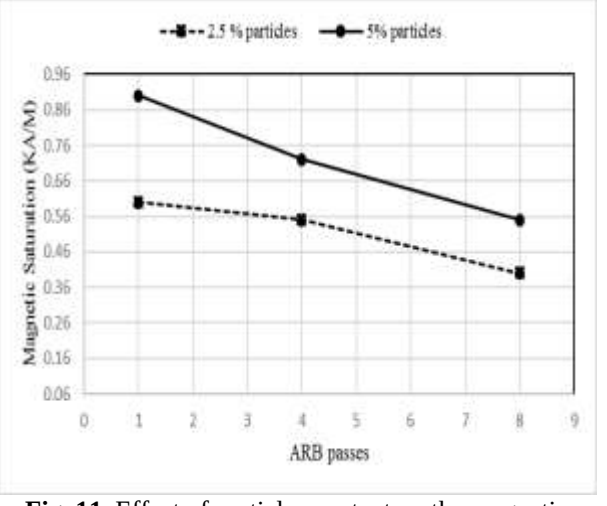

Fig. 11. Effect of particles content on the magnetic saturation of composites fabricated after the 8th pass.

4. CONCLUSION

- At higher number of ARB passes the uniformity of Fe_2O_3 particles through the Al matrix increases which has an essential effect on the uniformity of the magnetic saturation.
- Increasing the ARB passes improves the mechanical properties of composite samples by means of the enhancement of strength and elongation due to the dynamic crystallization.
- Hysteresis curves for all of composite samples show an increasing rate for Magnetic residual and coercivity h_c with increasing the Fe_2O_3 particles value at higher number of ARB passes.
- The magnetic saturation value increases by increasing the number of layers at higher number of ARB process.

REFERENCES

[1] M Sedighi, MH Vini, P Farhadipour, "**Effect of alumina content on the mechanical properties of AA5083/Al2O3 composites fabricated by warm accumulative roll bonding,** " *Powder Metallurgy and Metal Ceramics*, Vol. 55 (7), pp. 413-418, 2016.

[2] M. Heydari Vini, M. Sedighi, "**Mechanical properties and bond strength of bimetallic AA1050/AA5083 laminates fabricated by Warm-Accumulative Roll Bonding**," *Canadian metallurgical quarterly*, Vol. 57, pp. 169-167, 2018.

[3] M. Sedighi, P. Farhadipour, M. Heydari Vini, "**Mechanical properties and microstructural evolution of bimetal 1050/Al2O3/5083 composites fabricated by warm accumulative roll bonding,** " *JOM*, Vol. 68 (12), pp. 3193-3200, 2016.

[4] Baniya, H. B., Guragain, R. P., Subedi, D. P. "**Cold atmospheric pressure plasma technology for modifying polymers to enhance adhesion: A critical review,**" *Reviews of Adhesion and Adhesives*, Vol.9(2), pp.269-307, 2021

[5] Brown, P., & Mazumder, P. "**Current Progress in Mechanically Durable Water- Repellent Surfaces: A Critical Review**," *REVIEWS OF ADHESION AND ADHESIVES*, Vol. 9(1), pp.123-152, 2021.

[6] Müssig, J., & Graupner, N. "**Test Methods for Fibre/Matrix Adhesion in Cellulose Fibre- Reinforced Thermoplastic Composite Materials: A Critical Review. Rev**," *Adhesion Adhesives*, Vol. 8, No. 2, pp.68-129, 2021.

[7] Rakshe, S., Nimje, S. V., & Panigrahi, S. K. "**Optimization of Adhesively Bonded Spar- Wingskin Joints of Laminated FRP Composites Subjected to Pull- Off Load: A Critical Review,**" *Reviews Of Adhesion And Adhesives*, Vol. 8(1), pp.29-46, 2021.

[8] Ghasemvand, M., Behjat, B., & Ebrahimi, S. "**Experimental investigation of the effects of adhesive defects on the strength and creep behavior of single-lap adhesive joints at various temperatures**," *The Journal of Adhesion*, pp.1-17. 2022.

[9] T. Zolfaghari, Z. Rafiee, "**Preparation and study of surface modified ZnO nanoparticles in copoly (amid-imide) nanocomposite films containing triptycene**," *J. Synth. Chem.*, Vol. 1, 108-115. 2022

[10] M. Shojaie, "**One-pot Multicomponent synthesis of pyrano[2,3-c]pyrazoles catalyzed by Copper oxide nanoparticles (CuO NPs),**" *J. Synth. Chem*. 2022, 1, 125-131. Doi: 10.22034/jsc.2022.155286

[11] Radhy, N., Jasim, L. "**A novel economical friendly treatment approach: Composite hydrogels**," *Caspian Journal of Environmental Sciences*, Vol.19(5), pp.841-852. 2021.

[12] Mansouri, M., Nademi, M., "**Ebrahim Olya, M., Lotfi, H. Study of Methyl tert-butyl Ether (MTBE) Photocatalytic Degradation with UV/TiO2-ZnO-CuO Nanoparticles**," *Journal of Chemical Health Risks*, Vol.7(1), pp.19-32. 2017.

[13] Dehghani Ashkezari, H., H. Sid Kalal, H. Hoveidi, M. R. Almasian, and M. Ashoor. "**Fabrication of UV/TiO2 nanotubes/Pd system by electrochemical anodization for furfural photocatalytic degradation**," *Caspian Journal of Environmental Sciences*, Vol.15, No. 1, pp. 1-11.2017.

[14] Ahmed, H. I., Abdulrahman, N. A. "**Effect of magnetic field on the preparation of Cu doped zinc oxide nanostructures in different temperatures**," *Eurasian Chemical Communications*, Vol. 3(7), pp. 443-451. 2021.

[15] Bozorgian, A., Zarinabadi, S., & Samimi, A. "**Preparation of Xanthan Magnetic Biocompatible Nano-Composite for Removal of Ni^2+ from Aqueous Solution,**" *Chemical Methodologies*, Vol.4(4), pp. 477-493.2010.

[16] MH Vini, M Sedighi, M Mondali, "**Mechanical properties, bond strength and microstructural evolution of AA1060/TiO2 composites fabricated**

by warm accumulative roll bonding (WARB)," *International Journal of Materials Research*, Vol.108 (1), pp. 53-59.2017

[17] Dehghani, N., Babamoradi, M., Hajizadeh, Z., Maleki, A. "**Improvement of Magnetic Property of CMC/Fe3O4 Nanocomposite by Applying External Magnetic Field During Synthesis**," *Chemical Methodologies*, Vol.4(1), pp.92-99. 2010.

[18] Khakyzadeh, V., Rezaei-Vahidian, H., Sediqi, S., Azimi, S. B., Karimi-Nami, R. "**Programming Adsorptive Removal of Organic Azo Dye from Aqueous Media Using Magnetic Carbon Nano-Composite**," *Chemical Methodologies*, Vol. 5(4), pp.324-330. 2021.

[19] Moghadam Ziabari, S. A., Babamoradi, M., Hajizadeh, Z., Maleki, A. "**The effect of magnetic field on the magnetic property of Agar/Fe3O4 nanocomposite**," *Eurasian Chemical Communications*, Vol.2(4), pp.456-464. 2020.

[20] Dehghan, M., Tahmasebipour, M., Ebrahimi, S. "**Design, fabrication, and characterization of an SLA 3D printed nanocomposite electromagnetic micro actuator**," Microelectronic Engineering, Vol. 254, pp.111695. 2022.

[21] Dwijendra, N.K.A., Patra, I., Ahmed, Y.M. et al. "**Carbonyl sulfide gas detection by pure, Zn- and Cd-decorated AlP nano-sheet,**" *Monatsh Chem (2022).* https://doi.org/10.1007/s00706-022-02961-5

[22] P Farhadipour, M Sedighi, MH Vini, "**Using warm accumulative roll bonding method to produce Al-Al2O3 metal matrix composite**, " *imeche part B*, Vol. 231 (5), pp. 889-896. 2017.

[23] M Heydari Vini, M Sedighi, M Mondali, "**Investigation of bonding behavior of AA1050/AA5083 bimetallic laminates by roll bonding technique**," *Transactions of the Indian Institute of Metals* 71 (9), pp. 2089-2094.2018.

[24] MH M. Sedighi, P. Farhadipour, "**Influence of temperature of accumulative roll bonding on the mechanical properties of AA5083/1% Al2O3 composite,**" *powder metalurgy and metal ceramics*, Vol. 56 (9-10),pp.496-503, 2018.

[25] M Heydari Vini, M Sedighi, M Mondali, "**Mechanical properties and microstructural evolution of AA5083/Al2O3 composites fabricated by warm accumulative roll bonding**," *ADMT Journal*, Vol. 9 (4), pp.13-22.2016.

[26] Shang, Y., Dehkordi, R. B., Chupradit, S., Toghraie, D., Sevbitov, A., Hekmatifar, M., Sabetand, R. "**The Computational Study of Microchannel Thickness Effects on H2O/CuO Nanofluid Flow with Molecular Dynamics Simulations**," *Journal of Molecular Liquids*, pp.118240. 2021.

[27] Panchal, H., Sadasivuni, K. K., Ahmed, A. A. A., Hishan, S. S., Doranehgard, M. H., Essa, F. A., Khalid, M. "**Graphite powder mixed with black paint on the absorber plate of the solar still to enhance yield: An experimental investigation**," *Desalination*, Vol. 520, 115349. 2021

[28] Salimi, M., Pirouzfar, V. Kianfar, E. "**Enhanced gas transport properties in silica nanoparticle filler-polystyrene nanocomposite membranes**," Colloid Polym Sci., Vol. 295, pp. 215–226. 2017.

[29] Salimi, M., Pirouzfar, V. & Kianfar, E. "**Novel nanocomposite membranes prepared with PVC/ABS and silica nanoparticles for C2H6/CH4 separation**," *Polym. Sci. Ser. A*, Vol. 59, pp.566–574. 2017.

[30] M.H. Vini, S. Daneshmand, "**Investigation of bonding properties of Al/Cu bimetallic laminates fabricated by the asymmetric roll bonding techniques**", *Advances in computational design*, Vol. 4 (1), pp. 33-41.2019.

[31] Y Gao, M.H. Vini, S. Daneshmand, AA Alameri, O Benjeddou, RHC Alfilh, "**Effect of Processing Parameters on Wear Properties of Hybrid AA1050/Al2O3/TiO2 Composites**," *Crystals*, Vol. 13 (2), pp. 335. 2023.

[32] MH Vini, S Daneshmand, "**Bonding evolution of bimetallic Al/Cu laminates fabricated by asymmetric roll bonding**," *Advances in materials research*: *AMR*, Vol. 8 (1), pp. 1-10. 2019.

[33] MH Vini, OH Zadeh , "**Significant enhancement of bond strength in the roll bonding process using Pb particles**", *Journal of Materials Research*, Vol. 109 (1), pp. 42-49. 2018.